MMSE Equalization for Aeronautical Telemetry Channels

MMSE EQUALIZATION FOR AERONAUTICAL TELEMETRY CHANNELS

Michael Rice
Brigham Young University

Md. Shah Afran
Mohammad Saquib
The University of Texas at Dallas

ABSTRACT

This paper presents performance analysis of the minimum mean squared error (MMSE) equalizers applied to aeronautical telemetry channels. The challenge for equalizing received samples of the modulated signal lies in the fact that the underlying continuous-time SOQPSK-TG waveform is not wide-sense stationary. However it is assumed so in order to meet real-time implementation requirements. Two approximations of the autocorrelation function of the SOQPSK-TG waveform are used for designing MMSE equalizers. Their performance are investigated against the zero forcing equalizer for measured aeronautical telemetry channels.

INTRODUCTION

The propagation of the radio signal from an airborne transmitter to a ground-based receiver over multiple paths may cause multipath interference. Usually, one of the paths is the line-of-sight propagation path whereas the others are due to reflections. Multipath interference continues to be the dominant cause of link outages in aeronautical telemetry. In this paper we investigate a data-aided approach to equalization assuming iNET packet structure. In data-aided equalization, the equalizer filter coefficients may be computed from the multipath channel coefficients.

iNET-formatted transmissions include a 128-bit preamble and 64-bit attached sync marker (ASM) preceding a block of data bits (at least 6144 bits: an LDPC codeword): see Figure 1. Since the preamble and ASM bits are known, the receiver can compare the received signal to a locally

Approved for public release; distribution is unlimited. 412TW-PA-14300

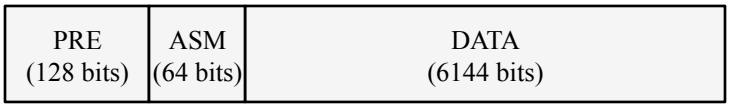

Figure 1: The iNET packet structure used in this paper.

stored copy of the SOQPSK-TG signal corresponding to the preamble and ASM bit fields. This comparison is capable of producing estimates of the frequency offset, noise variance, and multipath channel coefficients [4]. The multipath channel coefficient estimates can then be used to obtain equalizer filter coefficients.

The minimum mean-squared error (MMSE) filter coefficients depend on multipath channel coefficients, autocorrelation function of the SOQPSK-TG waveform and noise variance. Unfortunately, SOQPSK-TG waveform is not wide-sense stationary which results in time-varying filter coefficients and makes MMSE equalizer practically very difficult to realize. This situation leads us to make two approximations of the autocorrelation function of the SOQPSK-TG waveform and investigate their performance against the zero forcing (ZF) equalizer for measured aeronautical telemetry channels.

SYSTEM-LEVEL DESCRIPTION

The bit sequence for iNET is depicted in Figure 1. The preamble sequence (PRE) is CD98_{hex} repeated eight times [5, p. 48]. The preamble field is followed by the attached sync marker (ASM) field defined as $\text{034776C7272895B0}_{\text{hex}}$. The DATA field is 6144 randomized data bits.[1] The iNET bit sequence is modulated by SOQPSK-TG waveform which propagates through a frequency selective channel and experiences a frequency offset as well as the addition of additive white Gaussian noise.

The received signal is filtered, down-converted to I/Q baseband, and sampled (not necessarily in that order) using standard techniques. The resulting sequence of received samples is

$$r(n) = \left[\sum_{k=-N_1}^{N_2} h(k)s(n-k) \right] e^{j\omega_0 n} + w(n), \tag{1}$$

where $h(n)$ is the impulse response of the equivalent discrete-time channel with support on $-N_1 \leq n \leq N_2$, ω_0 rads/sample is the frequency offset, and $w(n)$ is a complex-valued zero-mean Gaussian random process with variance σ_w^2.

The focus of this paper is on equalizing the I/Q baseband samples of the received signal (1). Prior to applying the equalization techniques multiple tasks need to be performed by the receiver as shown in Figure 2. The preamble and ASM bits are known and thus the samples corresponding to those bits are used to estimate the frequency offset, channel impulse response, and, for the MMSE

[1] These bits correspond to a single LDPC codeword in the coded system. Here, we evaluate the uncoded bit error rate (BER) after equalization.

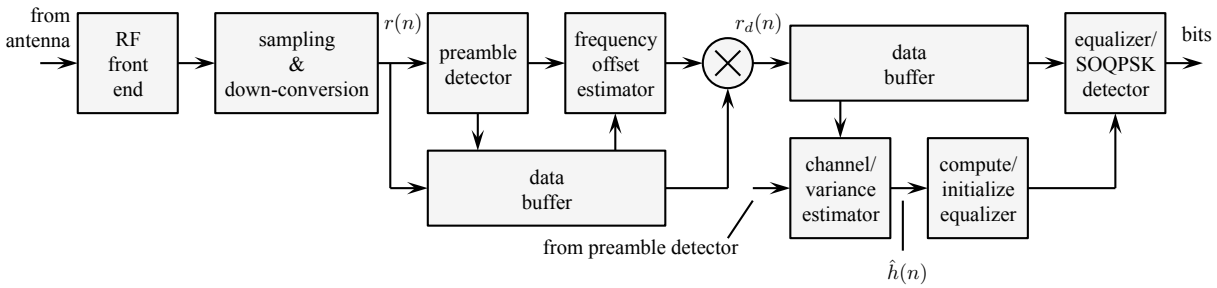

Figure 2: The data packet format and high-level signal processing explored in this paper.

equalizer, the noise variance. Before these estimations can be performed, the start of the samples corresponding to the preamble bits in the received signal must be detected. This is accomplished by the preamble detector block, whose algorithm is based on the detection algorithm described in [7]. Once the start of the preamble is known, the frequency offset is estimated using the algorithms described in [4]. The frequency offset is used with a complex-exponential to derotate the received data to remove the frequency offset. The derotated data $r_d(n)$ are used to estimate the channel and noise variance as described in [4]. The channel estimates $\hat{h}(n)$, for $-N_1 \leq n \leq N_2$, are then used to compute the MMSE and ZF equalizer filter coefficients.

THE EQUALIZATION ALGORITHMS

Since SOQPSK-TG is a nonlinear modulation, the equalizer cannot operate on the symbols in the same way it does for linear modulation (cf., [6, Chapter 9]). Consequently, the equalizer must operate on the samples of SOQPSK-TG, similar to the way fractionally spaced equalizers operate. The equalizers operate in the system configuration shown in Figure 3 [cf., Figure 2]. Here, the derotated samples $r_d(n)$ are equalized using a length $L_1 + L_2 + 1$ FIR filter defined by the impulse response $c(n)$ for $-L_1 \leq n \leq L_2$ to produce the output

$$y(n) = \sum_{m=-L_1}^{L_2} c(m) r_d(n-m). \tag{2}$$

The equalizer output forms the input to the well-known symbol-by-symbol SOQPSK detector comprising a detection filter operating at $N = T_b/T$ samples/bit and a decision process, operating on the decision variable $u(k)$ at 1 sample/bit. This detector, based on an offset QPSK approximation of SOQPSK-TG, is described in more detail in [8, 9]. The detectors of Figure 3 also include a phase lock loop (PLL). The PLL is required to track out any residual phase increments due to frequency offset estimation errors. A timing loop is not required because timing offsets are part of the channel estimate $\hat{h}(n)$. Now we will organize the MMSE equalizer filter coefficients into

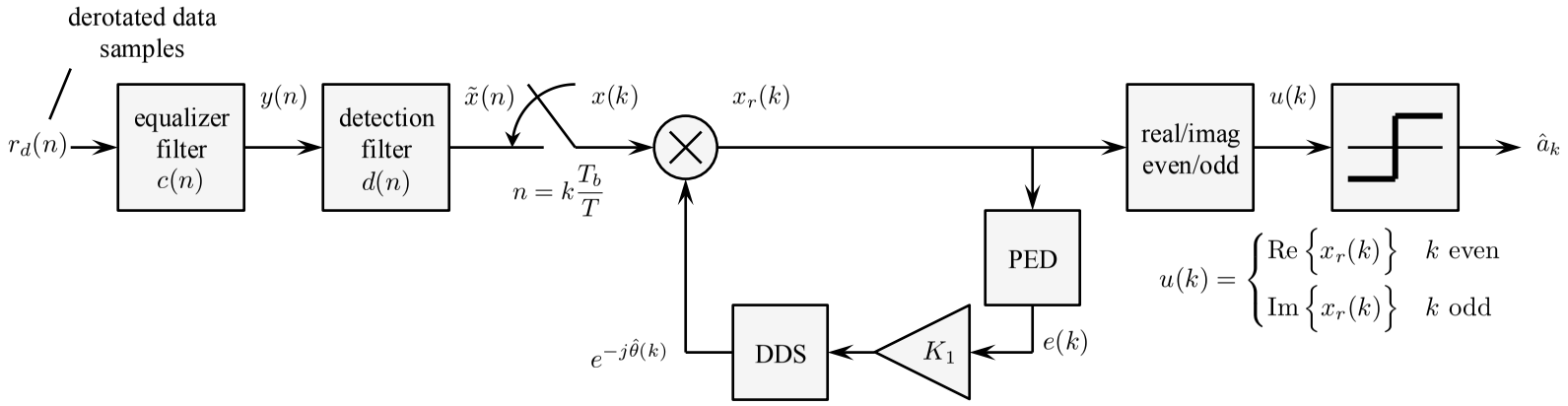

Figure 3: Block diagrams of the systems used in this paper for the ZF and MMSE equalizers.

$(L_1 + L_2 + 1) \times 1$ vectors as follows:

$$\mathbf{c}_{\text{MMSE}} = \begin{bmatrix} c_{\text{MMSE}}(-L_1) \\ \vdots \\ c_{\text{MMSE}}(0) \\ \vdots \\ c_{\text{MMSE}}(L_2) \end{bmatrix}. \tag{3}$$

The MMSE equalizer is a filter that minimizes the mean squared error

$$\mathcal{E} = \mathrm{E}\left\{ \left| s(n) - r_d(n) * c(n) \right|^2 \right\}. \tag{4}$$

As mentioned earlier, the challenge with equalizing *samples* of the modulated signal is that the underlying continuous-time waveform is not wide-sense stationary [6]. This fact carries over by the autocorrelation function of $s(n)$

$$R_s(k, \ell) = \frac{1}{2}\mathrm{E}\left\{ s(k)s^*(\ell) \right\}. \tag{5}$$

Notice in (5) that the autocorrelation function is a function of both sample indexes, not the difference between them. Consequently, the equalizer filter coefficients are a function of the sample index n. It is hard to see how this solution has any practical utility, especially in the presence of a real-time performance requirement. In the end, the designer is left with suboptimal approaches of reduced computational complexity whose accompanying performance penalty is acceptable.

The simplest suboptimal approach is to assume that the signal samples are wide-sense stationary. Here, the autocorrelation function is of the form

$$R_s(k - \ell) = \frac{1}{2}\mathrm{E}\left\{ s(k)s^*(\ell) \right\}, \tag{6}$$

that is, the autocorrelation function depends on the difference of the sample time indexes. The wide-sense stationary assumption for $s(n)$ greatly simplifies the solution. Because the equalizer coefficients no longer depend on the samples index n, the relationship between $s(n)$ and the equalizer output $\hat{s}(n)$ is

$$\hat{s}(n) = c(n) * r_d(n) = \sum_{m=-L_1}^{L_2} c(m) r_d(n - m). \tag{7}$$

Recall that $r_d(n)$ is the derotated version of the received samples. The vector of filter coefficients that minimizes the mean squared error

$$\mathcal{E} = \mathrm{E}\left\{ \left| s(n) - \hat{s}(n) \right|^2 \right\}, \tag{8}$$

is given by

$$\mathbf{c} = \left[\mathbf{G}\mathbf{R}_{s,1}\mathbf{G}^\dagger + \mathbf{R}_w \right]^{-1} \mathbf{R}_{s,2}\mathbf{g}^\dagger, \tag{9}$$

where $\mathbf{c}$ is the $(L_1 + L_2 + 1) \times 1$ vector of filter coefficients, $\mathbf{G}$ is the $(L_1 + L_2 + 1) \times (N_1 + N_2 + L_1 + L_2 + 1)$ matrix described by

$$\mathbf{G} = \begin{bmatrix} \hat{h}(N_2) & \cdots & \hat{h}(-N_1) & & \\ & \hat{h}(N_2) & \cdots & \hat{h}(-N_1) & \\ & & \ddots & & \\ & & & \hat{h}(N_2) & \cdots \quad \hat{h}(-N_1) \end{bmatrix}; \tag{10}$$

$\mathbf{R}_{s,1}$ is the $(L_1 + L_2 + N_1 + N_2 + 1) \times (L_1 + L_2 + N_1 + N_2 + 1)$ matrix given by

$$\mathbf{R}_{s,1} = \begin{bmatrix} R_s(0) & R_s(-1) & \cdots & R_s(-L_1 - L_2 - N_1 - N_2) \\ R_s(1) & R_s(0) & \cdots & R_s(-L_1 - L_2 - N_1 - N_2 + 1) \\ \vdots & & & \vdots \\ R_s(L_1 + L_2 + N_1 + N_2) & R_s(L_1 + L_2 + N_1 + N_2 - 1) & \cdots & R_s(0) \end{bmatrix}; \tag{11}$$

$\mathbf{R}_w$ is the $(L_1 + L_2 + 1) \times (L_1 + L_2 + 1)$ noise autocorrelation matrix given by

$$\mathbf{R}_w = \begin{bmatrix} R_w(0) & \cdots & R_w(-L_1 - L_2) \\ \vdots & & \vdots \\ R_w(L_1 + L_2) & \cdots & R_w(0) \end{bmatrix}; \tag{12}$$

$\mathbf{R}_{s,2}$ is the $(L_1 + L_2 + 1) \times (L_1 + L_2 + 1)$ matrix given by

$$\mathbf{R}_{s,2} = \begin{bmatrix} R_s(0) & R_s(-1) & \cdots & R_s(-L_1 - L_2) \\ R_s(1) & R_s(0) & \cdots & R_s(-L_1 - L_2 + 1) \\ \vdots & & & \vdots \\ R_s(L_1 + L_2) & R_s(L_1 + L_2 - 1) & \cdots & R_s(0) \end{bmatrix}; \tag{13}$$

and $\mathbf{g}$ is the $1 \times (L_1 + L_2 + 1)$ vector given by

$$\mathbf{g} = \begin{bmatrix} \hat{h}(L_1) & \cdots & \hat{h}(-L_2) \end{bmatrix}, \tag{14}$$

where it is understood that $h(n) = 0$ for $n < -N_1$ or $n > N_2$ (how many zeros need to be prepended and appended depends on the relationship between L_1 and N_2 and the relationship between L_2 and N_1).

The question is now, what function should be used for the autocorrelation function $R_s(k)$? Two approximations are investigated here. The first is an empirically-derived autocorrelation function. The empirical autocorrelation function is obtained by generating a large number of samples $s(n)$ and using the standard estimation technique assuming wide sense stationarity. Given L samples of $s(n)$ for $n = 0, 1, \ldots, L-1$, this empirical autocorrelation function is

$$R_{\mathrm{e}}(k) = \frac{1}{2(L-k)} \sum_{n=k}^{L-1} s(n) s^*(n-k), \qquad 0 \le k < L - 1 \tag{15}$$

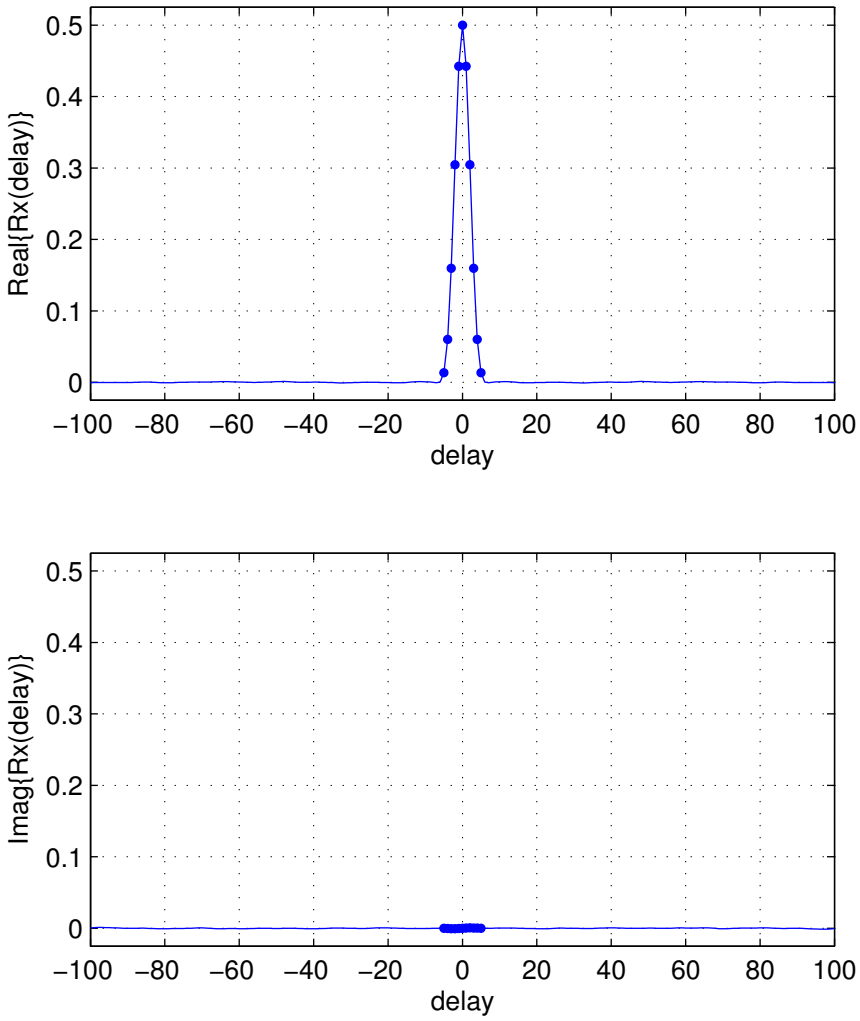

Figure 4: A plot of the empirical autocorrelation function for SOQPSK-TG: (top) the real part of $R_{\rm e}(k)$; (bottom) the imaginary part of $R_{\rm e}(k)$. The sample rate for the SOQPSK-TG samples is at 2 samples/bit. Markers indicate the values for $-5 \leq k \leq 5$.

together with

$$R_{\rm e}(k) = R_{\rm e}^*(-k), \qquad -L < k < 0. \tag{16}$$

A plot of $R_{\rm e}(k)$ corresponding to $L = 2 \times 10^6$ samples of SOQPSK-TG sampled at 2 samples/bit is shown in Figure 4 for the first 100 lags (i.e., $-100 \leq k \leq 100$). The top plot shows the real part of $R_{\rm e}(k)$ and the lower plot shows the imaginary part of $R_{\rm e}(k)$. The only significant values are those for $-5 \leq k \leq 5$ and indicated by markers on the plot. Consequently, in the simulation results presented below, we assume $R_{\rm e}(k) = 0$ for $|k| > 5$.

The second approximation is to assume the data are uncorrelated. This generates a correlation function of the form

$$R_{\rm i}(k) = \sigma_s^2 \delta(k). \tag{17}$$

Here, the corresponding correlation matrices $\mathbf{R}_{s,1}$ and $\mathbf{R}_{s,2}$ are scaled identity matrices and they

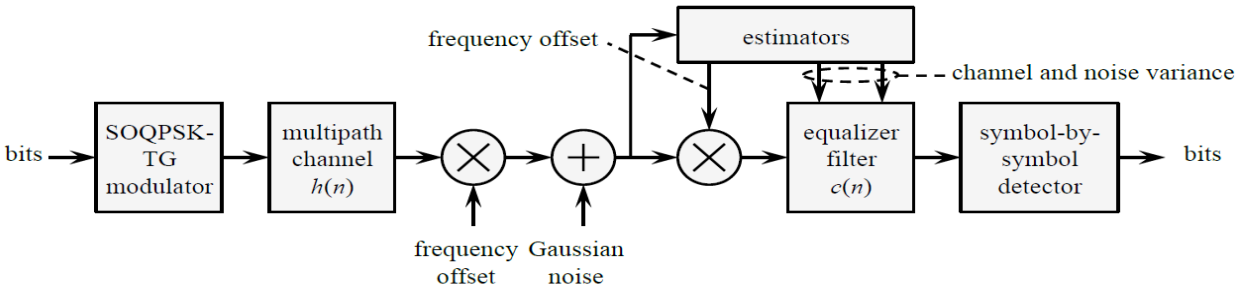

Figure 5: A block diagram of the simulation procedure.

function as regularizers in the numerical computations (9).The solution is given by a form of the Wiener-Hopf equations [10]. The $(L_1 + L_2 + 1) \times 1$ vector of MMSE equalizer filter coefficients are

$$\mathbf{c}_{\text{MMSE}} = \left[\mathbf{G}\mathbf{G}^{\dagger} + \frac{\hat{\sigma}_w^2}{\sigma_s^2}\mathbf{I}_{L_1+L_2+1}\right]^{-1} \mathbf{g}^{\dagger}, \tag{18}$$

where $\mathbf{G}$ is the $(L_1 + L_2 + 1) \times (N_1 + N_2 + L_1 + L_2 + 1)$ matrix as described in (10), $\mathbf{g}$ is the $1 \times (L_1 + L_2 + 1)$ vector as described in (14) and σ_s^2 is the signal power. This solution is based on the assumption that SOQPSK-TG samples corresponding to a sample rate of 2 samples/bit are approximately uncorrelated. The ZF equalizer is a filter that is the best length-$(L_1 + L_2 + 1)$ FIR approximation to the "inverse" of the channel. Its filter coefficients can be derived from (18) by letting noise variance $\hat{\sigma}_w^2 = 0$.

PERFORMANCE RESULTS

The BER performance of the equalization techniques was assessed using the simulation environment outlined in Figure 5. The simulation parameters were the following:

1. The payload data rate was equivalent to 10 Mbits/s (the equivalent "over-the-air" bit rate was 10.3125 Mbits/s). The iNET-formatted SOQPSK-TG signal and channel were generated at an equivalent sample rate of 2 samples/bit.

2. Because the channel estimator does not know the true length of the channel, the estimator used values for N_1 and N_2 larger than any of the test channels. These values were $N_1 = 12$ and $N_2 = 25$ samples.

3. The equalizers used $L_1 = 4 \times N_1 = 48$ samples and $L_2 = 4 \times N_2 = 100$ samples. Thus the length of equalizer filter was 149 samples.

4. The simulations were performed over 10 representative channels derived from channel sounding measurements conducted at Edwards AFB under the M4A program [12]. The test channels are summarized in Table 1 and the corresponding frequency-domain plots are shown in Figure 6.

Table 1: Description of the ten test channels used in the simulations.

channel	N_1	N_2	length	environment
01	1	7	9	Taxiway E
02	2	17	20	Taxiway E
03	1	22	24	Taxiway E
04	5	13	19	Takeoff on 22L
05	1	1	3	Cords Road
06	1	2	4	Cords Road
07	0	4	5	Cords Road
08	2	3	6	Black Mountain
09	1	1	3	Black Mountain
10	2	3	6	Land on 22L

The simulated BER performance is shown in Figures 7 – 11. In all cases we observe that both versions of the MMSE equalizer exhibit almost identical performance, which is noticeably better than the performance of the ZF for most of the channels except channels 6 and 9. This is to be expected because test channels 6 and 9 are rather benign [see Figure 6]. Similarly, when the channel has deep and wide spectral nulls in the middle of the spectrum of SOQPSK-TG waveform, MMSE equalizer is expected to provide significant gain over the ZF equalizer. In Figure 8 for channel 4, it can be noticed that at a target BER = 10^{-5} both MMSE equalizers yield about 3 dB signal-to-noise ratio gain over the ZF equalizer. The fact that the ZF equalizer has such performance is not surprising. The ZF equalizer simply "inverts the channel" (this phrase derives from the frequency domain point of view). For channels with nulls, the "inversion" restores the frequency content of the desired signal in the frequency band surrounding the null. This restoration also amplifies the noise power in the same frequency band. The end result is a phenomenon known as "noise amplification:" the distortion due to the multipath channel is corrected at the cost of reduced signal-to-noise ratio. In contrast an MMSE equalizer takes a more measured approach to "channel inversion" and balances the impact of residual multipath distortion and amplified noise on cost functions [mean squared error (4) for the MMSE equalizer]. Again, from the plots of simulated BER we observe that there is essentially no difference in the performance between the two versions of the MMSE equalizer. Consequently, $R_{\mathrm{i}}(k)$ is preferable over $R_{\mathrm{e}}(k)$ because this choice simplifies the computations of the equalizer filter coefficients.

CONCLUSIONS

This paper demonstrated the effectiveness of the MMSE equalizers against the ZF eqalizer with iNET-formatted SOQPSK-TG over measured aeronautical telemetry channels. SOQPSK-TG waveform is not wide-sense stationary. However, the real-time implementation of the MMSE equalizer led us to assume the underlying continuous waveform as a wide-sense stationary process. To further simplify the computational complexity of the equalizer coefficients we assumed that the

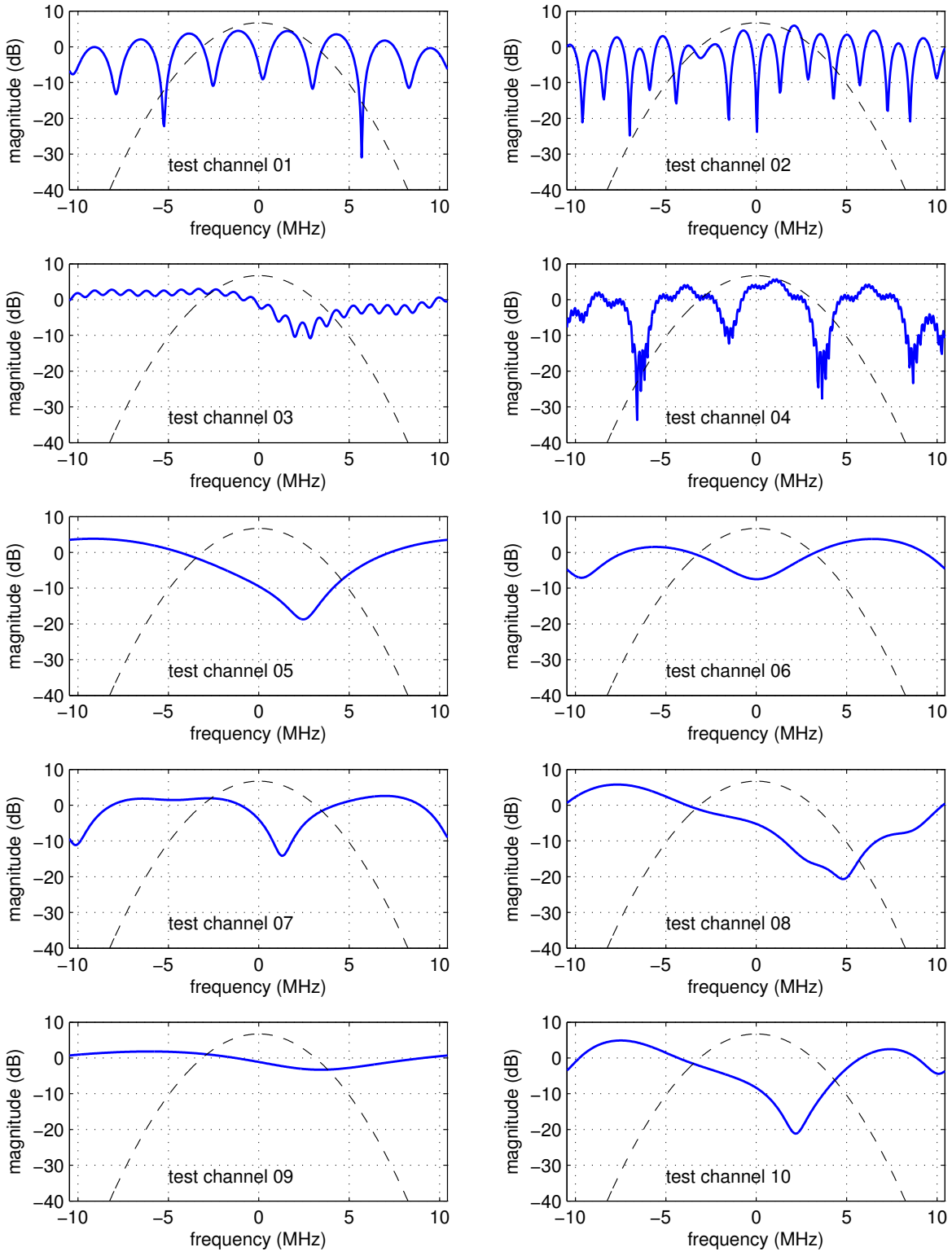

Figure 6: Frequency-domain plots of the example channels from channel sounding experiments at Edwards AFB. In each plot, the thick line is the channel frequency response and the thin line is the power spectral density of SOQPSK-TG operating at 10.3125 Mbits/s.

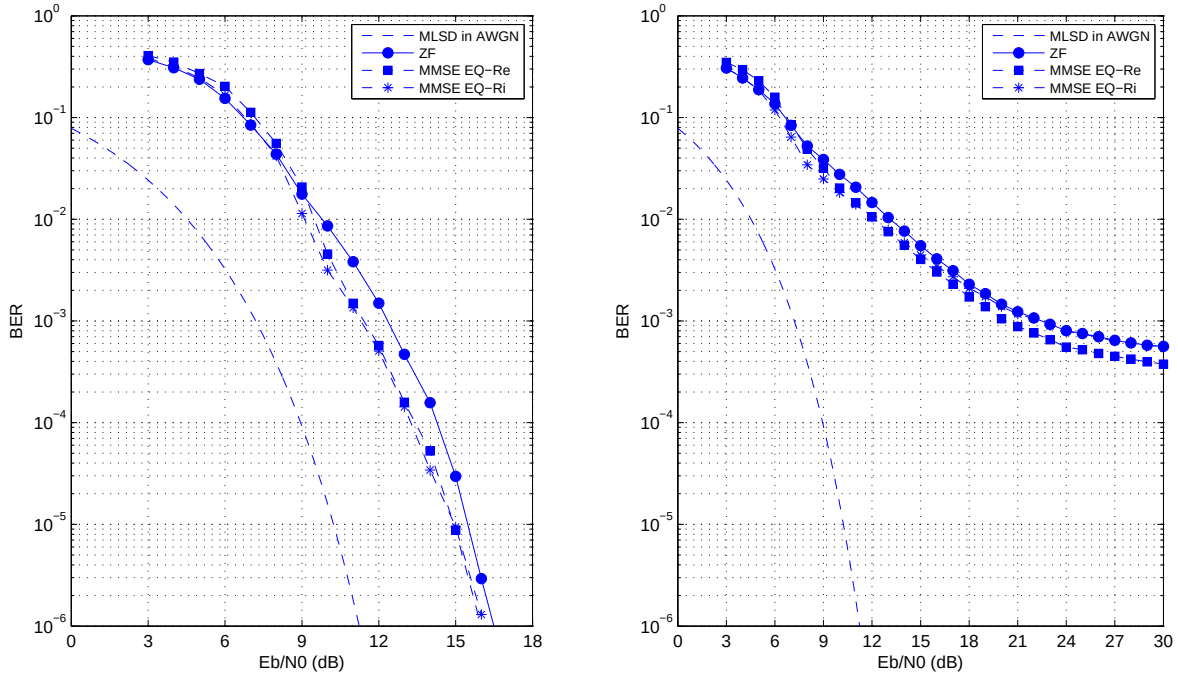

Figure 7: Simulation results for test channel 1 (left) and test channel 2 (right).

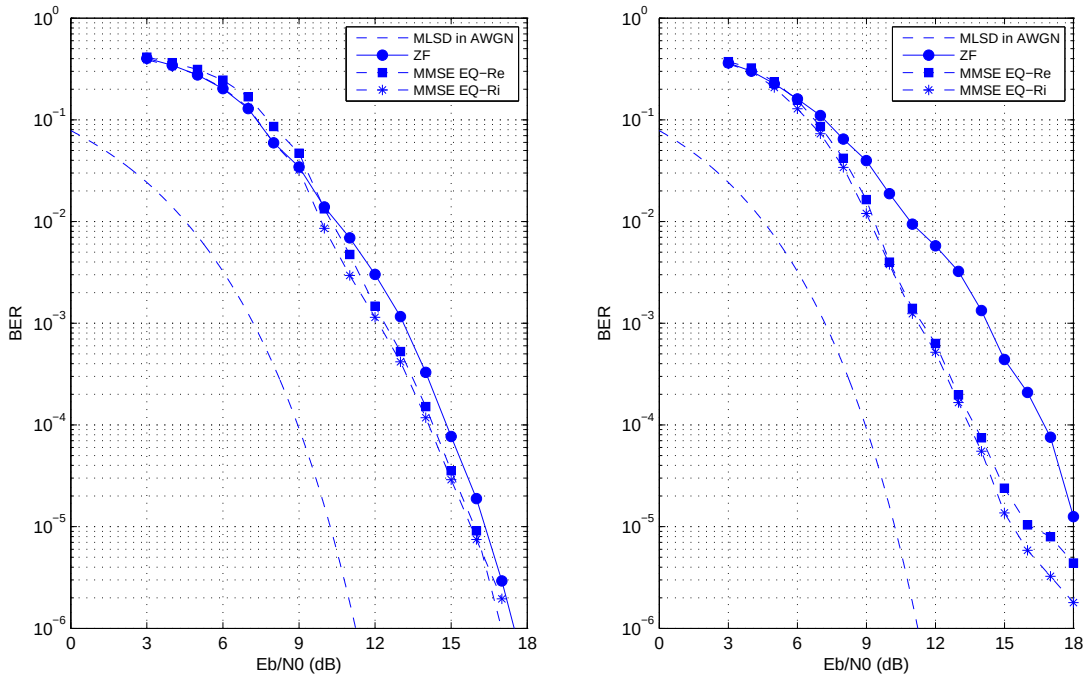

Figure 8: Simulation results for test channel 3 (left) and test channel 4 (right).

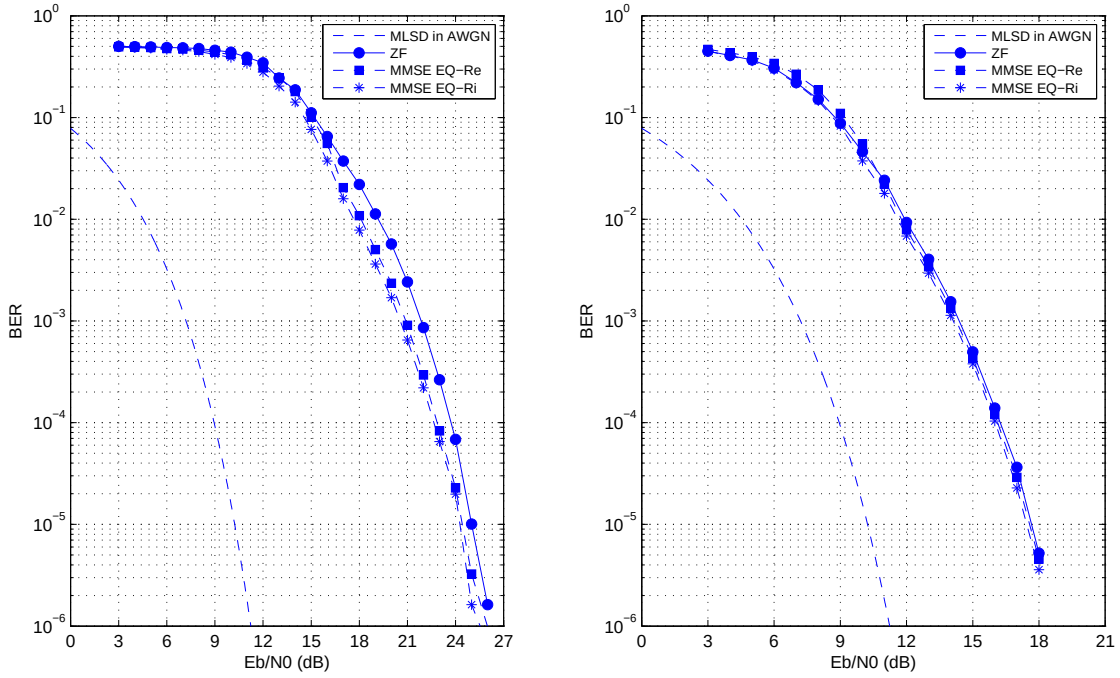

Figure 9: Simulation results for test channel 5 (left) and test channel 6 (right).

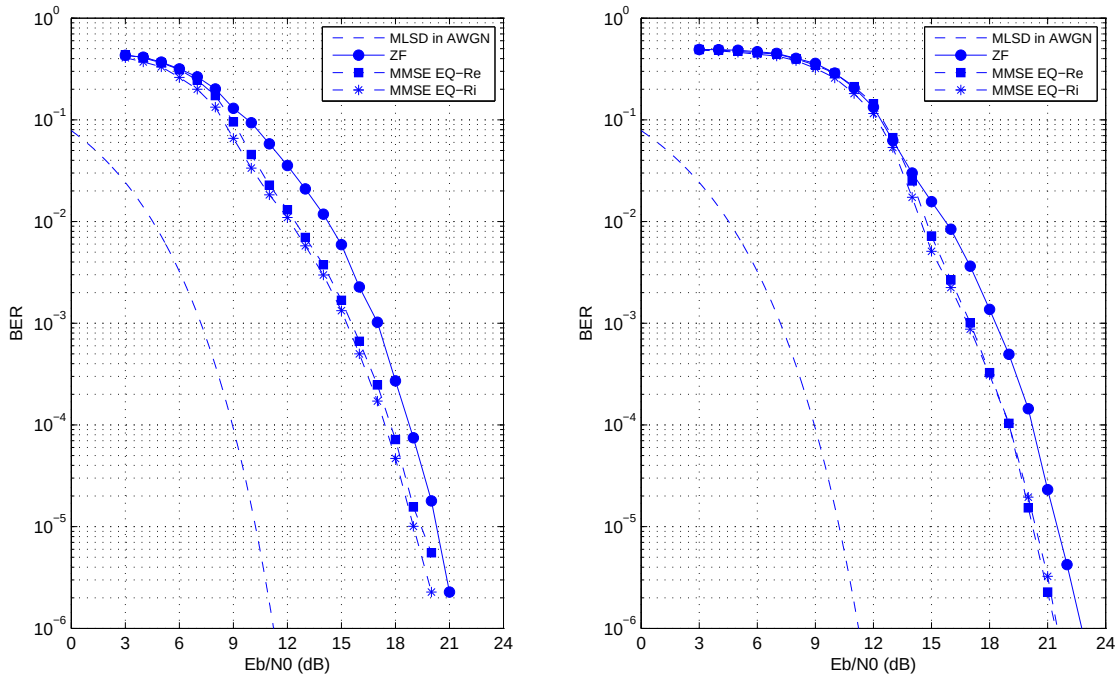

Figure 10: Simulation results for test channel 7 (left) and test channel 8 (right).

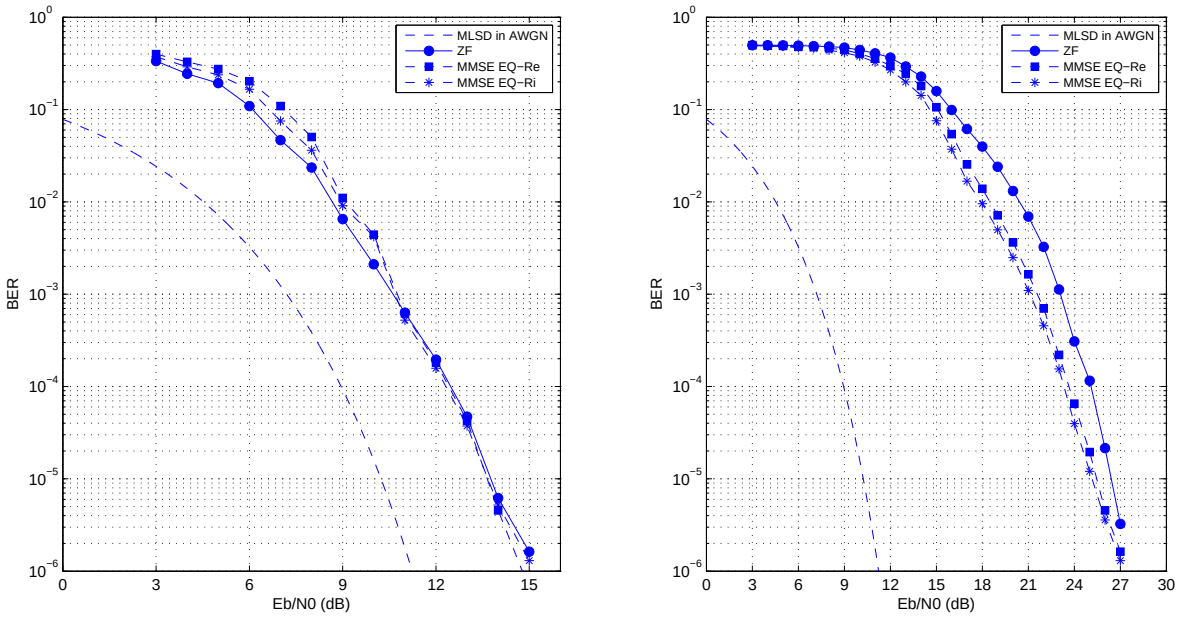

Figure 11: Simulation results for test channel 9 (left) and test channel 10 (right).

waveform was not only wide-sense stationary but also uncorrelated. Our numerical results showed that this simplification did not penalize the system in terms of BER and depending on the channel, at a target BER = 10^{-5} MMSE equalizers were capable of providing $0 - 3$ dB signal-to-noise ratio gain over the ZF equalizer.

ACKNOWLEDGEMENTS

This work was funded by the Test Resource Management Center (TRMC) Test and Evaluation Science and Technology (T&E/S&T) Program through the U.S. Army Program Executive Office for Simulation, Training and Instrumentation (PEO STRI) under contract W900KK-13-C-0026 (PAQ).

REFERENCES

[1] Z. Ye, E. Satorius, and T. Jedrey, "Enhancement of advanced range telemetry (ARTM) channels via blind equalization," in *Proceedings of the International Telemetering Conference*, Las Vegas, NV, October 2001.

[2] T. Hill and M. Geoghegan, "A comparison of adaptively equalized PCM/FM, SOQPSK, and multi-h CPM in a multipath channel," in *Proceedings of the International Telemetering Conference*, San Diego, CA, October 2002.

[3] M. Geoghegan, "Experimental results for PCM/FM, Tier I SOQPSK, and Tier II Multi-h CPM with CMA equalization," in *Proceedings of the International Telemetering Conference*, Las Vegas, NV, October 2003.

[4] M. Rice, M. Saquib, and E. Perrins, "Estimators for iNET-formatted SOQPSK-TG," in *Proceedings of the the International Telemetering Conference*, San Diego, CA, October 2014.

[5] integrated Network Enhanced Telemetry (iNET) Radio Access Network Standards Working Group, "Radio access network (RAN) standard, version 0.7.9," Tech. Rep., available at `https://www.tena-sda.org/display/INET/iNET+Platform+Interface+Standards`.

[6] J. Proakis and M. Salehi, *Digital Communications*, 5th ed. New York: McGraw-Hill, 2008.

[7] A. McMurdie, M. Rice, and E. Perrins, "Preamble detection for iNET-formatted SOQPSK-TG," in *Proceedings of the the International Telemetering Conference*, San Diego, CA, October 2014.

[8] T. Nelson, E. Perrins, and M. Rice, "Near optimal common detection techniques for shaped offset QPSK and Feher's QPSK," *IEEE Transactions on Communications*, vol. 56, no. 5, pp. 724–735, May 2008.

[9] E. Perrins, "FEC systems for aeronautical telemetry," *IEEE Transactions on Aerospace and Electronic Systems*, vol. 49, no. 4, pp. 2340–2352, October 2013.

[10] M. Hayes, *Statistical Digital Signal Processing and Modeling*. New York: John Wiley & Sons, 1996.

[11] M. Rice, M. S. Afran, and M. Saquib, "Equalization in aeronautical telemetry using multiple antennas," submitted to *IEEE Transactions on Aerospace & Electronic Systems*, 2014.

[12] M. Rice and M. Jensen, "A comparison of L-band and C-band multipath propagation at Edwards AFB," in *Proceedings of the International Telemetering Conference*, Las Vegas, NV, October 2011.